GPS Solut (2017) 21:727–737
DOI 10.1007/s10291-016-0563-8

ORIGINAL ARTICLE

Basic performance of space-surface bistatic SAR using BeiDou satellites as transmitters of opportunity

Shuzhu Shi[1] · Jingnan Liu[2] · Tao Li[2] · Weiming Tian[3]

Received: 13 January 2016 / Accepted: 16 August 2016 / Published online: 22 August 2016

Abstract The basic performance of space-surface bistatic synthetic aperture radar (SS-BSAR) using BeiDou satellites as transmitters of opportunity is presented. The transmitted signal, the satellite trajectory, and the observation time are analyzed to demonstrate the potential of BeiDou satellites to be used as transmitters of SS-BSAR. When a BeiDou medium earth orbit (MEO) satellite is used, the signal-to-noise ratio and the resolution are examined for different SS-BSAR cases, where the receiver is fixed on the ground or mounted on a moving platform. Since the parameters of the BeiDou geostationary earth orbit (GEO) satellite and the inclined geosynchronous satellite orbit (IGSO) satellite are different from those of the MEO satellite, the peculiarities of SS-BSAR with the GEO or IGSO satellite as transmitter are analyzed and then compared with the case of MEO satellite. In order to show the performance difference of SS-BSAR with BeiDou satellites as transmitters, comparisons with other global navigation satellite system (GNSS) transmitters are also made. The theoretical results show that SS-BSAR using BeiDou satellites as transmitters can achieve different sounding performance and can provide some new potential applications compared to other GNSS transmitters.

✉ Shuzhu Shi
shuzhushi@hotmail.com

[1] School of Remote Sensing and Information Engineering, Wuhan University, Luoyu Road No. 129, Wuhan 430079, China

[2] Research Center of GNSS, Wuhan University, Luoyu Road No. 129, Wuhan 430079, China

[3] School of Information and Electronics, Beijing Institute of Technology, Zhongguancun South Street No. 5, Beijing 100081, China

Keywords BeiDou satellites · Radar signal analysis · Signal-to-noise ratio · Space-surface bistatic synthetic aperture radar · Synthetic aperture radar

Introduction

Over the last two decades, the global navigation satellite system (GNSS) signals have been used to sense the earth's environment. In addition to the application known as GNSS-reflectometry (Jin et al. 2011), the signals also have been proposed by Cherniakov (2002) to be used as transmitted signals of bistatic synthetic aperture radar for passive imaging; this system is referred to as the space-surface bistatic synthetic aperture radar (SS-BSAR). Many studies have been reported to demonstrate its performance with GPS, GLONASS, and the European Galileo system as transmitters of opportunity (Lazarov et al. 2013; Saini et al. 2008; Antoniou et al. 2013). For SS-BSAR with BeiDou satellites as transmitters, Ye et al. (2011) have used software simulations to demonstrate its imaging feasibility for a geostationary earth orbit (GEO) satellite and an airborne receiver, Zeng et al. (2015) have carried out several multiangle observation experiments for a medium earth orbit (MEO) satellite and a stationary receiver, and proposed a region-based image fusion method to improve image quality greatly. However, when BeiDou satellites were used as the transmitters of SS-BSAR, the characteristics of them have rarely been analyzed, such as the transmitted signal, the satellite trajectory, and the observation time. Actually, these characteristics are important for research on potential performance of SS-BSAR and specification of its application area. In addition, in contrast to other GNSS systems where only the MEO satellites are included, the

GEO and the inclined geosynchronous satellite orbit (IGSO) satellites are also included in the BeiDou system. Compared with the MEO satellite, the GEO and IGSO satellites have different orbit altitude, satellite trajectory, and observation time. When the latter two types of satellites are used as the transmitters of SS-BSAR, the system configuration, the signal processing algorithm, and the sounding performance may be different from the case of MEO satellites. However, very few studies are focused on SS-BSAR with the BeiDou GEO or IGSO satellite as transmitter. Moreover, compared with other GNSS satellites, the performance difference of SS-BSAR with BeiDou satellites as transmitters has not been reported yet.

We first analyze the transmitted signal, the satellite trajectory, and the observation time for the BeiDou satellites. Next, we examine the signal-to-noise ratio (SNR) of SS-BSAR with the BeiDou MEO satellite as transmitter for different configurations. This is followed by comparisons with the SNR of SS-BSAR using BeiDou GEO and IGSO satellites or other GNSS satellites as transmitters, including a focus on the range and azimuth resolution of SS-BSAR. Toward the end we verify the theoretical performance of SS-BSAR with the BeiDou IGSO satellite as transmitter via a simulation.

Characteristics of BeiDou satellites

In order to demonstrate the potential of BeiDou satellites as transmitters of SS-BSAR, an analysis of their characteristics is presented, including the transmitted signal, the satellite trajectory, and the observation time. Furthermore, the differences between the BeiDou MEO satellite and the GEO or IGSO satellite are highlighted.

Transmitted signal

The signals of the BeiDou satellites presently available are listed in Table 1 (Montenbruck et al. 2013). Taking into account the service type and to achieve better range resolution, the B3 in-phase (I) component can be chosen as the transmitted signal of SS-BSAR to obtain a potentially range resolution of about 15 m. Mathematically, the BeiDou B3 signal can be written as

$$S(t) = A_{\mathrm{I}}C_{\mathrm{I}}(t)D_{\mathrm{I}}(t)\cos(2\pi f_{\mathrm{c}}t + \phi) + A_{\mathrm{Q}}C_{\mathrm{Q}}(t)D_{\mathrm{Q}}(t)\sin(2\pi f_{\mathrm{c}}t + \phi) \quad (1)$$

where A_{I}(or A_{Q}),$C_{\mathrm{I}}(t)$(or $C_{\mathrm{Q}}(t)$), and $D_{\mathrm{I}}(t)$(or $D_{\mathrm{Q}}(t)$) denote the amplitude, the ranging code, and the navigation message of the I component [or the quadrature (Q) component], respectively, f_{c} denotes the carrier frequency, and ϕ is the initial phase. In practical operation, only $C_{\mathrm{I}}(t)$ is used for the purpose of imaging, and the effects produced by $D_{\mathrm{I}}(t)$ and the B3 Q component can be suppressed with the method described by Saini et al. (2010). Therefore, both of them will be neglected in the subsequent signal analysis for simplicity.

According to the Woodward ambiguity function (Woodward 1953), the three-dimensional (3-D) ambiguity function $|\chi(\tau, v)|$, the delay autocorrelation function $|\chi(\tau, 0)|$, and the Doppler autocorrelation function $|\chi(0, v)|$ are shown for the BeiDou B3 I component in Fig. 1, where τ is the delay, v is the Doppler shift, and T denotes the width of one chip. In this simulation, a 66-bit ranging code is adopted due to the limited performance of the used computer, but the results obtained are very similar for the ranging code whose length is 10,230 bits.

The top panel of Fig. 1 shows that there is a sharp peak in the center of the ambiguity function. This implies that the BeiDou B3 I component has good delay and Doppler resolution, and can be used as the transmitted signal of SS-BSAR. Furthermore, the middle panel shows that the range peak sidelobe level is −13.47 dB, and hence, a sidelobe suppression filter should be added in the imaging algorithm. The bottom panel shows that the Doppler autocorrelation function has a sinc-shaped form, and the Doppler peak sidelobe level is −13.26 dB.

Table 1 Available signals of BeiDou satellites (Montenbruck et al. 2013)

Band	Central frequency/ MHz	Chip rate/ Mcps	Service type
B1(I)	1561.098	2.046	Open
B1(Q)	1561.098	2.046	Authorization
B2(I)	1207.140	2.046	Open
B2(Q)	1207.140	10.23	Authorization
B3(I)	1268.520	10.23	Civil Authorization
B3(Q)	1268.520	10.23	Authorization

Satellite trajectory

Trajectories of the BeiDou satellites with respect to a building (30.53°N, 114.36°E) located at Wuhan University on January 25, 2013 are shown in Fig. 2. The top panel shows the location of four BeiDou MEO satellites. They are not stationary relative to the earth's surface, and their trajectories show a pattern similar to that of other GNSS MEO satellites. Therefore, when these satellites used as the transmitter, SS-BSAR has the same system configuration as other GNSS transmitters (He et al. 2005). The middle panel shows five BeiDou GEO satellites which lie in the south and are almost stationary relative to the earth's surface. When they are used as the transmitter of SS-BSAR, the receiver should be mounted on a moving platform, and

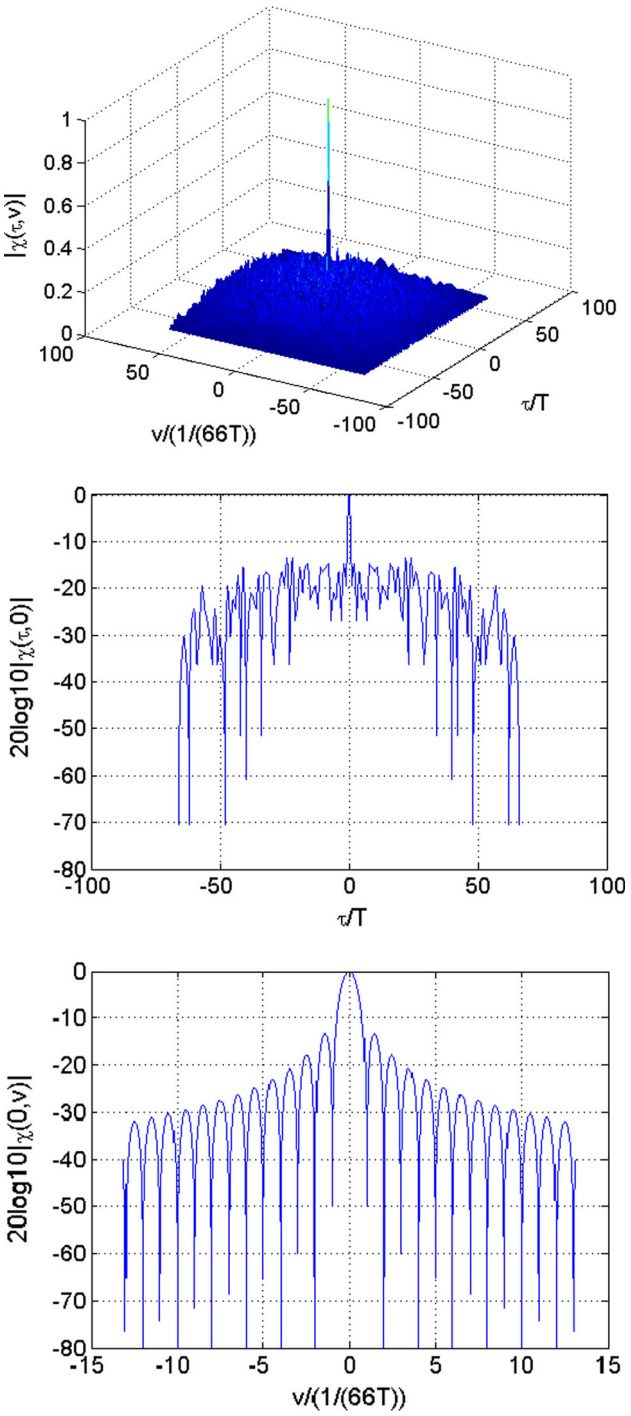

Fig. 1 3-D ambiguity function (*top*), delay autocorrelation function (*middle*), and Doppler autocorrelation function (*bottom*) of the BeiDou B3 I component. The axes labels τ/T denotes the delay normalized by delay resolution T, $v/(1/(66\,T))$ denotes the Doppler shift normalized by Doppler resolution $1/(66\,T)$, $20\log 10|\chi(\tau,0)|$ and $20\log 10|\chi(0,v)|$ denote the log scale of delay and Doppler autocorrelation function

the aperture synthesis is provided by motion of the receiver. Since we only have to consider the motion of the platform and considering that its trajectory is

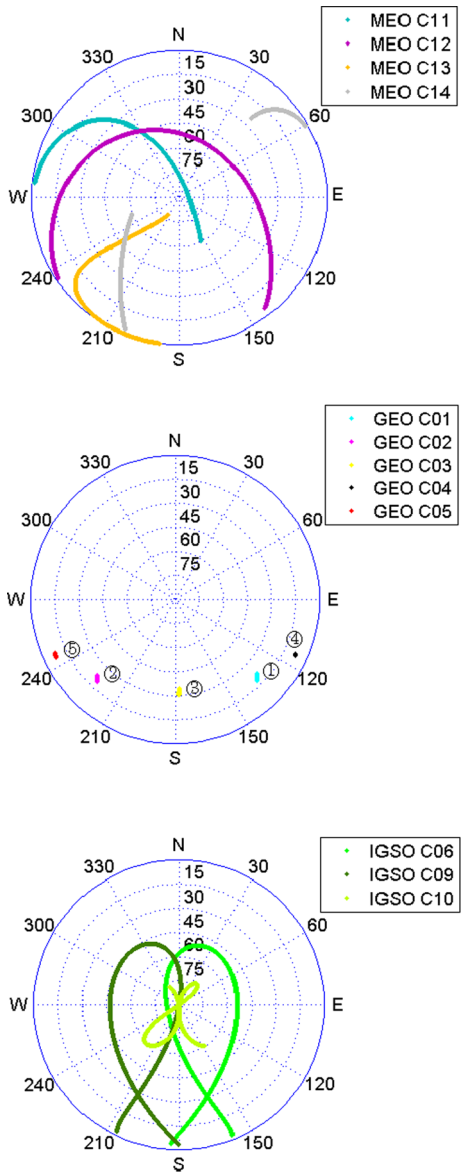

Fig. 2 Trajectories of the four BeiDou MEO satellites (*top*), five GEO satellites (*middle*), and three IGSO satellites (*bottom*) with respect to a building located at Wuhan University on January 25, 2013. The IGSO C07 and C08 have the same trajectories as the IGSO C06

approximately linear, the current BSAR imaging algorithms operating in the azimuth–frequency domain are directly applicable to this case. The bottom panel shows that five BeiDou IGSO satellites are also not stationary relative to the earth's surface, but their trajectories are a repeated "figure-8"-shaped ground track and are different from those of the MEO satellites. Therefore, when the IGSO satellite is adopted as the transmitter of SS-BSAR, the system configuration is similar to that of the MEO satellite case, but the correction of the satellite trajectory in the imaging algorithm will be different.

Observation time

The available BeiDou satellites at Wuhan University on January 25, 2013, are shown in Fig. 3, where the x-axis is the observation time in hours, the sampling interval is 30 s, and the y-axis is the satellite PRN. This figure shows that the BeiDou GEO and IGSO satellites can provide longer observation time than the MEO satellite, and the GEO satellites are visible around the clock. Therefore, if the full observation time can be processed, SS-BSAR with the BeiDou GEO or IGSO satellite as transmitter may achieve larger processing gain and finer azimuth resolution than in case of MEO satellite. Moreover, the GEO and IGSO satellites are potentially better for permanent and continuous monitoring of the important targets.

Analysis of SNR

According to the classical radar equation (Skolnik 1990), the SNR of SS-BSAR using a BeiDou MEO satellite as transmitter is analyzed for different configurations to show its potential operational range. Furthermore, comparisons are made to show the peculiarities of SS-BSAR using the BeiDou GEO or IGSO satellite. In addition, comparisons with other GNSS satellites are also made to show the different sounding performance when the BeiDou satellites are employed.

SNR in case of a BeiDou MEO satellite and a moving receiver

When the receiver is mounted on a moving platform and the aperture synthesis is only provided by the platform motion, the equation for calculating the SNR can be derived as

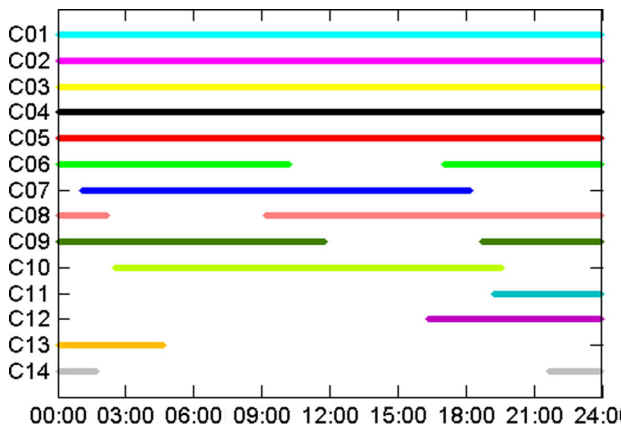

Fig. 3 Availability of the BeiDou satellites at Wuhan University on January 25, 2013

$$\mathrm{SNR} = \rho_{\mathrm{pfd}} \times \sigma \frac{A_{\mathrm{R}}}{4\pi R_{\mathrm{Rt}}} \times \frac{\tau_i}{kT_0F_n} \times \frac{\mathrm{PRF} \times \lambda}{V_{\mathrm{a}}\delta_{\mathrm{az}}}\eta \tag{2}$$

where ρ_{pfd} represents the power flux density near the earth's surface produced by the BeiDou satellites, σ is the radar cross section (RCS) of a single target with strong reflection coefficient, which is supposed to be independent of frequency and angle, A_{R} is the effect area of the receiving antenna, R_{Rt} is the range between the receiver and the target, τ_i denotes the uncompressed signal duration, k is the Boltzmann constant $1.38 \times 10^{-23}\mathrm{W\,s/^{\circ}K}$, T_0 is the thermal noise temperature of the receiving system 290°K, F_n is the noise factor of the receiver, PRF denotes the pulse repetition frequency in the azimuth dimension, λ is the wavelength, V_{a} is the velocity of the platform, δ_{az} is the azimuth resolution, and η is the loss factor.

In practical operation of SS-BSAR, PRF is usually set to $1/\tau_i$, F_n is considered to be 1 dB, and η is assumed to be $\eta = 0.5$. When the BeiDou B3 I component is used as the transmitted signal and a receiving antenna with 13 dB gain is adopted, we get $\lambda \approx 0.23633\,\mathrm{m}$ and $A_{\mathrm{R}} \approx 0.08889\,\mathrm{m}^2$. Moreover, when the elevation angle of the BeiDou satellite is above 5°, the minimum power received by a 0-dB omni-directional antenna is -163 dBW (BeiDou 2013). Therefore, the minimum value of ρ_{pfd} is equal to $1.1276 \times 10^{-14}\,\mathrm{W/m^2}$. In addition, since the potential azimuth resolution of SS-BSAR is equal to the horizontal aperture of the receiving antenna, δ_{az} can be considered to be 1 m. In terms of the aforementioned parameter values, Eq. (2) can be rewritten as

$$\mathrm{SNR} = 1870.7625 \times \frac{\sigma}{R_{\mathrm{Rt}}V_{\mathrm{a}}} \tag{3}$$

If the receiver is mounted on an unmanned aerial vehicle (UAV), we can get $V_{\mathrm{a}} \approx 50\mathrm{m/s}$. According to (3), the variation in the SNR with R_{Rt} for different values of σ is shown in the top panel of Fig. 4. It can be observed that if 10 dB SNR is considered as the detection threshold of SS-BSAR, a target with 100 m^2 RCS can only be detected at a range of about 374 m.

Let us now consider another configuration, i.e., the aperture synthesis is provided by the motions of platform and satellite. In this case, T_{dt} denotes the dwell time over which the target is simultaneously covered by the beam of the transmitting and receiving antennas. As a result, the equation used to calculate the SNR can be written as

$$\mathrm{SNR} = \rho_{\mathrm{pfd}} \times \sigma \frac{A_{\mathrm{R}}}{4\pi R_{\mathrm{Rt}}^2} \times \frac{\tau_i}{kT_0F_n} \times (\mathrm{PRF} \times T_{\mathrm{dt}})\eta \tag{4}$$

Since the MEO satellite illuminate a large part of the earth's surface with the global beam, T_{dt} is mainly decided by the beamwidth of the receiving antenna, and it can be expressed as

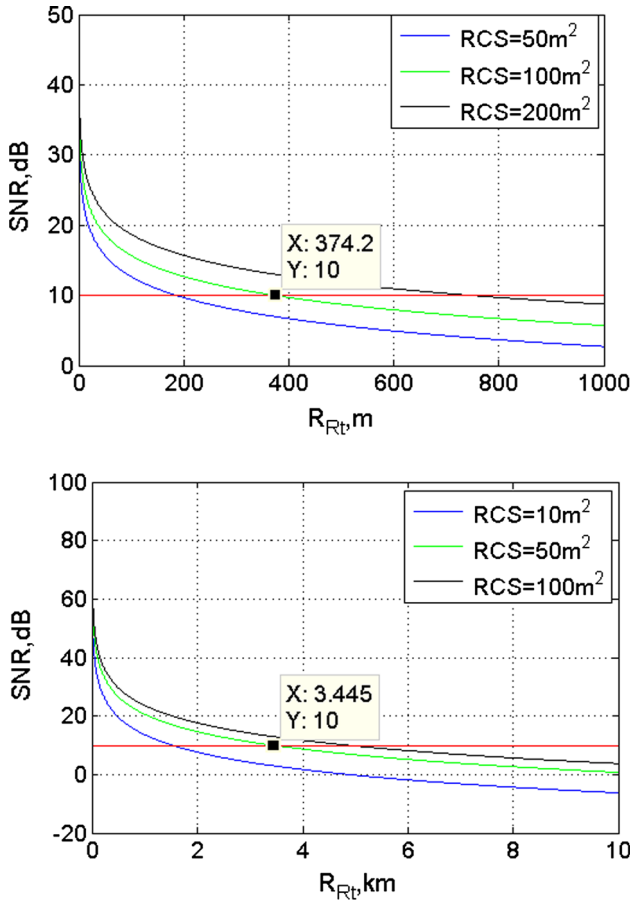

Fig. 4 Variation in the SNR with R_{Rt} for different values of RCS in case of BeiDou MEO satellite and an airborne receiver (*top*) or a stationary receiver (*bottom*)

$$T_{dt} \approx \frac{\lambda R_{Rt}}{V_a \delta_{az}} \tag{5}$$

Substituting (5) into (4), it can be found that the SNR obtained in this configuration has almost the same value as the one where the aperture synthesis is only provided by the platform motion.

SNR in case of a BeiDou MEO satellite and a stationary receiver

When the receiver is fixed on the ground, the aperture synthesis is only provided by the motion of the BeiDou MEO satellite, and the equation used to calculate the SNR can be written as

$$\mathrm{SNR} = \rho_{\mathrm{pfd}} \times \sigma \frac{A_R}{4\pi R_{Rt}^2} \times \frac{\tau_i}{kT_0 F_n} \times \frac{\mathrm{PRF} \times \lambda \times R_{Tt}}{V_s \delta_{az}} \eta \tag{6}$$

where V_s is the speed of the satellite, and R_{Tt} is the range between the satellite and the target. It can be seen that the difference between (2) and (6) lies in the dwell time T_{dt}.

If $T_{dt} = 300$ s, just like the value of dwell time used in a practical imaging experiment (Antoniou et al. 2012), then (6) can be simplified as

$$\mathrm{SNR} = 2.375 \times 10^6 \times \frac{\sigma}{R_{Rt}^2} \tag{7}$$

In terms of (7), the variation in the SNR with R_{Rt} for different values of σ is given in the bottom panel of Fig. 4, and it can be seen that if 10 dB SNR is set as the detection threshold of SS-BSAR, a target with 50 m^2 RCS can be detected at the range of approximately 3.4 km. A comparison between the panels of Fig. 4 shows that SS-BSAR with the stationary receiver can achieve higher SNR than in case of a moving receiver, due to an essentially longer target dwell time. As presented in (5), when the receiver is mounted on an UAV and $R_{Rt} = 3.446$ km, T_{dt} is approximately equal to 16 s. However, when the aperture is provided by the satellite motion, the minimum value of T_{dt} is much larger than 16 s because of the large transmitting beam of the illuminating satellite.

Comparison with SNR in case of BeiDou GEO or IGSO satellites

As mentioned earlier, when a BeiDou GEO satellite is used as the transmitter, the receiver should be mounted on a moving platform which provides the aperture synthesis. Regarding this configuration, T_{dt} is mainly decided by the beamwidth of the receiving antenna. If the same receiving antenna is adopted, the value of T_{dt} will remain unchanged compared to the MEO satellite case. In addition, although the orbit altitude of the GEO satellite is higher than that of the MEO satellite, SS-BSAR with the GEO satellite as transmitter can receive almost the same power, i.e., there is no change in the value of ρ_{pfd}. If the other parameters remain the same, Eq. (2) shows that SS-BSAR using a GEO satellite as transmitter can achieve the same SNR as from a MEO satellite.

Similarly, when the BeiDou IGSO satellite is used as the transmitter and the receiver is mounted on a moving platform, SS-BSAR also can achieve the same SNR as in case of a MEO satellite, whether the aperture synthesis is only provided by the motion of the platform or by the motion of platform and satellite. However, when the receiver is fixed on the ground and the aperture synthesis is provided by the motion of the satellite, since the BeiDou IGSO satellite has higher orbit altitude and longer observation time than the MEO satellite, a longer target dwell time can be potentially obtained. If other parameters remain the same, Eq. (6) shows that SS-BSAR using this satellite as the transmitter can achieve higher SNR than in case of the MEO satellite.

Table 2 Some parameters of the GNSS MEO satellites

Band	Central frequency (MHz)	Chip rate (Mcps)	Orbit altitude (km)	$\rho_{pfd}(\mathrm{W/m^2})$
BeiDou B3(I)	1268.52	10.23	21,528	1.1276×10^{-14}
GPS L1(C/A)	1575.42	1.023	20,180	2.7563×10^{-14}
GLONASS L1(P)	1603.6875	5.11	19,130	1.4322×10^{-14}
Galileo E5b(Q)	1207.140	10.23	23,222	4.0668×10^{-14}

Comparison with SNR in case of other GNSS satellites

In case MEO satellites from either GPS, GLONASS, or Galileo systems are used as transmitters, some respective parameters are listed in Table 2. We should mention that due to the service type of GNSS signals, we only consider the uncoded signals that had been reported to be used as the transmitted signals of SS-BSAR (Cherniakov et al. 2007).

When different GNSS MEO satellites are used and the receiver is mounted on the UAV, the variation in the SNR with R_{Rt} can be obtained in terms of (2) and is shown for a target with 400 m^2 RCS in the top panel of Fig. 5. Compared to the BeiDou MEO satellite, it shows that SS-BSAR using the Galileo or GPS satellite as transmitter can achieve higher SNR, especially the Galileo satellite. This is because larger ρ_{pfd} can be achieved with Galileo or GPS satellites. In addition, although a slightly larger ρ_{pfd} can be obtained with a GLONASS satellite, SS-BSAR using this satellite as transmitter has a lower SNR than in case of a BeiDou MEO satellite, because of its short wavelength.

On the other hand, when different GNSS MEO satellites are used as transmitters and the receiver is fixed on the ground, the variation in the SNR with R_{Rt} can be obtained in terms of (6) and is shown for a target with 50 m^2 RCS in the bottom panel of Fig. 5. We should state at this point that δ_{az} is considered to be 1 m. Compared to the BeiDou MEO satellite, it shows that SS-BSAR with the Galileo satellite as transmitter can achieve higher SNR, due to the larger value of ρ_{pfd} and the longer target dwell time. Furthermore, when the GPS satellite is used as the transmitter, almost the same SNR can be obtained. For the GLONASS satellite, however, the SNR is still significantly lower than that of the BeiDou MEO satellite case, because of its low wavelength and short target dwell time.

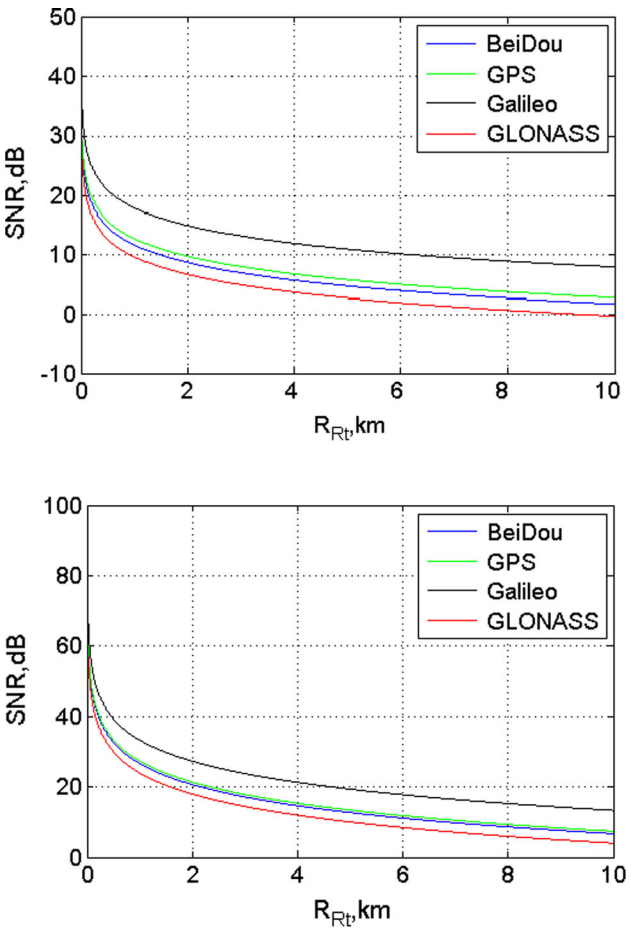

Fig. 5 Variation in the SNR with R_{Rt} for a target with 400 m^2 RCS and an airborne receiver (*top*) or for a target with 50 m^2 RCS and a stationary receiver (*bottom*), when different GNSS MEO satellites are used as the transmitters of SS-BSAR

Analysis of system resolution

According to the generalized ambiguity function, Zeng et al. (2005) have derived the expressions of the range and azimuth resolution for the BSAR in detail and have successfully applied them to clarify the performance of several BSAR systems. When GNSS satellites are used as the transmitters, these expressions can be written as

$$\delta_r = 0.583c/[2\cos(\beta/2)B] \tag{8}$$

$$\delta_{az} = \frac{0.886\lambda}{2\omega_S T_{\mathrm{dt}}} \tag{9}$$

where δ_r denotes the range resolution, B is the bandwidth of the transmitted signal, c is the speed of the light, β is the bistatic angle, and ω_S is the equivalent angular speed with respect to the target. Furthermore, other resolution parameters can be derived in terms of the range and

azimuth resolution, such as the ground resolution cell. Therefore, the range and azimuth resolution of SS-BSAR using the BeiDou MEO satellite as transmitter are first analyzed for different configurations. Comparisons are then made to show the unique resolution of the BeiDou GEO or IGSO satellite cases, and to show the resolution difference when compared with other GNSS transmitters.

Resolution in case of a BeiDou MEO satellite and a moving receiver

The 3-D geometry of SS-BSAR for this case is shown in the top panel of Fig. 6. The origin of the coordinate system is set as the nadir of the midpoint of the receiver's synthetic aperture, and the *x*–*O*–*y* plane coincides with the ground plane. The MEO satellite is moving along a direction parallel to the *y*-axis, with position specified by the coordinates $(x_{\mathrm{tr}}, y_{\mathrm{tr}}, z_{\mathrm{tr}})$ and velocity V_s. The receiver is moving along a nonparallel trajectory, with position specified by the coordinates $(0, 0, z_{\mathrm{re}})$ and velocity V_a. α is used here to specify the angle between the *x*-axis and the direction of the receiver velocity vector. The simulation parameters are listed in Table 3.

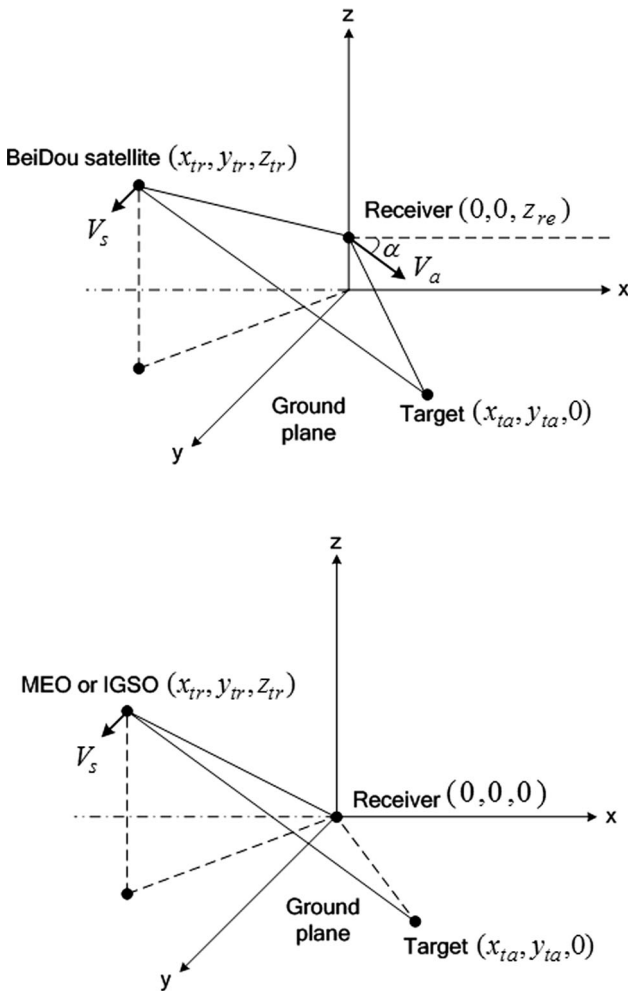

Fig. 6 3-D geometry of SS-BSAR in case of BeiDou satellites and an airborne receiver (*top*), and in case of BeiDou MEO or IGSO satellites and a stationary receiver (*bottom*)

Table 3 Simulation parameters when the BeiDou satellites are used as the transmitters of SS-BSAR

Item	Specification
Satellite altitude	MEO: 21,528 km; IGSO or GEO: 35,786 km
Satellite azimuth	120°
Satellite elevation	30°
Satellite speed	MEO: 3500 m/s; IGSO: 3000 m/s
Satellite motion direction	Parallel to the *y*-axis
Signal bandwidth	10.23 MHz
Total integration time	Airborne receiver: 38 s; Stationary receiver: 300 s
Airborne receiver speed	50 m/s
Airborne receiver altitude	5 km
Receiver motion direction	MEO or IGSO: $\alpha = 60^{\circ}$; GEO: $\alpha = 90^{\circ}$

In terms of (8) and (9), the simulated range and azimuth resolution results are shown in Fig. 7. In addition, when $\alpha = 90^{\circ}$, i.e., the satellite and the receiver have parallel paths, the corresponding azimuth resolution is also given for comparison. The top panel of Fig. 7 shows that the range resolution is not symmetric along the *y*-axis due to the asymmetric structure in such a configuration. Furthermore, a potential range resolution of 9 m can be obtained, because the illuminating satellite and the receiver are located at the same side of the target area to allow a small bistatic angle. When the position of the target changes from the upper part to the lower part of the *y*-axis, the range resolution becomes better due to the decreasing bistatic angle.

When the airborne receiver and the MEO satellite have parallel paths, the bottom panel shows that the azimuth resolution is symmetric along both the *x*-axis and the *y*-axis, because the moving direction of the receiver is parallel to the *y*-axis and the azimuth resolution is dominated by the receiver motion. Furthermore, when the target is located closer to the origin of the coordinate system, the azimuth resolution becomes finer due to the larger angular speed of the receiver with respect to the target. However, when the receiver and the MEO satellite have nonparallel paths, the middle panel shows that the azimuth resolution has a slightly different spatial variation, owing to the different direction of the receiver motion.

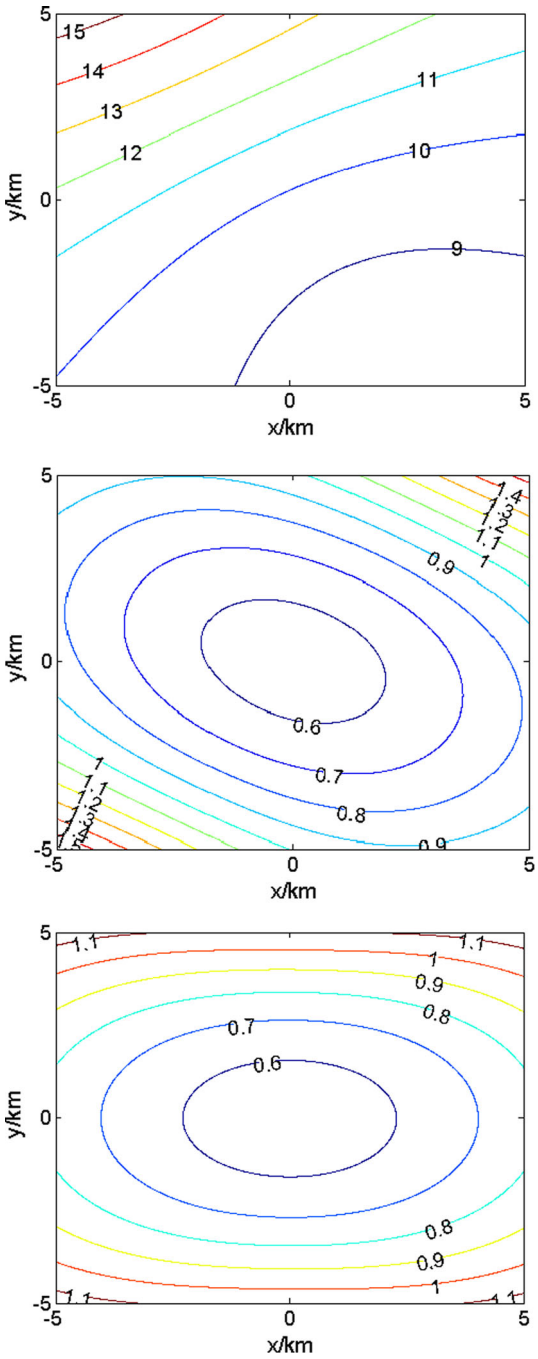

Fig. 7 Range resolution (*top*) and azimuth resolution of SS-BSAR when the satellite and the receiver have nonparallel (*middle*) or parallel paths (*bottom*) for the case of a BeiDou MEO satellite and an airborne receiver. The units of these contour numbers are meter

Resolution in case of a BeiDou MEO satellite and a stationary receiver

The 3-D geometry for this case is shown in the bottom panel of Fig. 6 and is similar to the top panel, except that the receiver is fixed on the ground, and its position is set as

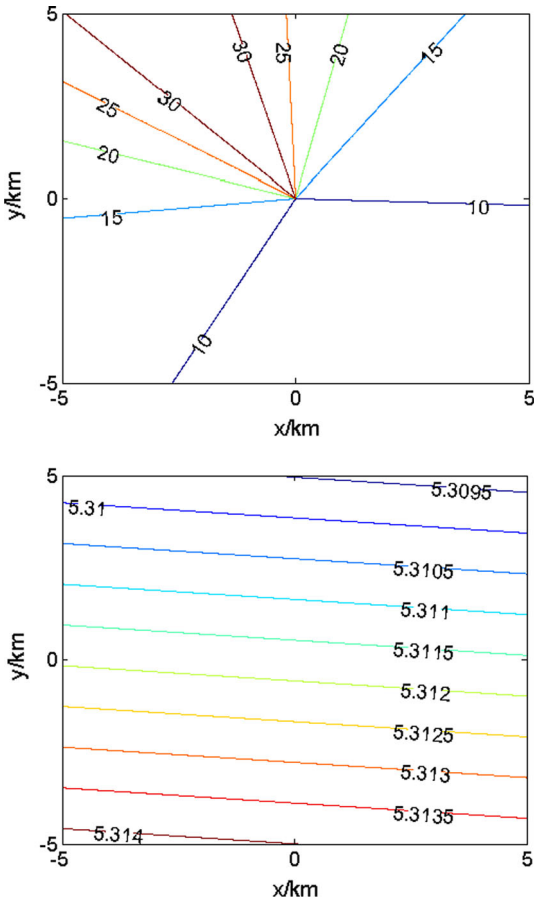

Fig. 8 Range (*top*) and azimuth (*bottom*) resolution of SS-BSAR for the case of a BeiDou MEO satellite and a stationary receiver. The units of these contour numbers are meter

the origin of the coordinate system. The simulation parameters are also listed in Table 3.

According to (8) and (9), the simulated range and azimuth resolution results in this case are shown in Fig. 8. The top panel shows that the range resolution of SS-BSAR with a stationary receiver has a spatial variation similar to the case of the moving receiver, because of the similar system configuration and the very high altitude of the satellite. The main difference lies in the azimuth resolution. The bottom panel shows that the azimuth resolution is about 5.3 km and is almost spatially invariant, following the fact that the azimuth resolution is dominated by the satellite motion, and the variation of the target position can only change the angular speed of the satellite slightly. It also shows that the lines have a light slope, because of the system geometry. In addition, a comparison between the bottom panels of Figs. 7 and 8 shows that although SS-BSAR with the stationary receiver can achieve longer target dwell time than the airborne receiver case, the azimuth resolution becomes worse due to the larger distance between the satellite and the target.

Comparison with resolution in case of BeiDou GEO or IGSO satellites

The 3-D geometry for the case of BeiDou GEO or IGSO satellites and an airborne receiver is shown in the top panel of Fig. 6, and the simulation parameters are listed in Table 3. The simulated results in this case are the same as these shown in Fig. 7. The same range resolution is due to the fact that for the configuration with such a high satellite altitude, although the altitude of the BeiDou GEO or IGSO satellite is higher than that of the MEO satellite, the bistatic angle will remain almost unchanged with further increase in the satellite altitude. In addition, the reason for the same azimuth resolution is that azimuth resolution is mainly determined by the receiver motion, and the receiver speed and motion direction are much the same for the two configurations.

On the other hand, owing to the same signal bandwidth and the almost unchanged bistatic angle, SS-BSAR consisting of IGSO satellite and a stationary receiver also can achieve the same range resolution as the case of MEO satellite. However, its azimuth resolution changes to be about 11.3 km because of the lower satellite speed and higher altitude, resulting in a slower angular speed with respect to the target. Nevertheless, it is important to mention that this comparison is made under the same integration time. In practice, longer integration time can be obtained with the IGSO satellite, and its azimuth resolution will be improved significantly.

Comparison with resolution in case of other GNSS satellites

When the MEO satellites in the GPS, GLONASS, and Galileo systems are used as the transmitters of SS-BSAR and the receiver is mounted on a moving platform, the 3-D geometry is similar to that shown in the top panel of Fig. 6. Moreover, the parameters listed in Table 2 are adopted, and other simulation parameters are similar to those listed in Table 3. Since the range resolution in such configurations is mainly determined by the signal bandwidth, SS-BSAR with the Galileo satellite as transmitter can achieve the same range resolution as the case of the BeiDou MEO satellite. However, the range resolution becomes worse in case of a GPS or GLONASS satellite. If satellite and receiver have nonparallel paths, since the azimuth resolution is mainly decided by the wavelength, SS-BSAR using a GLONASS or GPS satellite can achieve a finer azimuth resolution than the one consisting of BeiDou MEO satellite and an airborne receiver, especially for the GLONASS system. However, the azimuth resolution becomes worse in case of a Galileo satellite. Nevertheless, it should be noted that the difference among these results is small.

On the other hand, when the receiver is fixed on the ground, the range and azimuth resolution of SS-BSAR with other GNSS satellites as transmitters have the same spatial variation as the case of BeiDou MEO satellite, because of the similar configuration. Furthermore, the same results as in the case of a moving receiver can be obtained for the system resolution in this case, due to the fact that the range resolution is mainly determined by the signal bandwidth, and the azimuth resolution degrades with the increasing satellite altitude.

Simulation results

Since the SNR and the resolution of SS-BSAR with the MEO satellite as transmitter has been validated by previous research (Cherniakov et al. 2007), a simulation is performed here to briefly verify the theoretical performance of SS-BSAR consisting of a BeiDou IGSO satellite and a stationary receiver. To coincide with the conditions used for the theoretical performance analysis, the imaging geometry is the same as that shown in the bottom panel of Fig. 6, and the simulation parameters are the same as these listed in Table 3. Furthermore, a point target with 50 m^2 RCS is adopted, and its position is specified by coordinates (400, 200, 0 m). Note that its RCS is supposed to be independent of the illuminating angle. During the target dwell time, the signal $e(t,u)$ received from this point target, after baseband demodulation, can be modeled as

$$e(t,u) = P_e \times S\left[t - \frac{R_{\mathrm{Tt}}(u) + R_{\mathrm{Rt}}}{c}\right] \times \mathrm{rect}\left(\frac{u}{2T_{\mathrm{d}t}}\right) \times \exp\left\{-j2\pi f_{\mathrm{c}} \frac{R_{\mathrm{Tt}}(u) + R_{\mathrm{Rt}}}{\mathrm{c}}\right\} + n(t) \quad (10)$$

where $P_e = \frac{\rho_{\mathrm{pfd}} \times \sigma \times A_{\mathrm{R}}}{4\pi R_{\mathrm{Rt}}}$ is the power of the received signal, u denotes the azimuth time, and $n(t)$ represents the Gaussian white noise.

According to (10), the simulated images of this point target can be obtained with the bistatic back-projection algorithm and are shown in Fig. 9. From the top panel, the noise power is obtained by calculating the variance of the noise region, and the signal power is achieved from the square of the amplitude of the peak point in the signal region. As shown in the bottom panel, the range and azimuth resolution are obtained from the cross sections along the range and azimuth dimensions. In addition, a comparison between the theoretical and simulated results is listed in Table 4. Inspection of it shows a high level of similarity, suggesting the correctness of our theoretical results.

Conclusions and summary

The basic performance of SS-BSAR using BeiDou satellites as transmitters has been presented. Since some parameters of the BeiDou GEO and IGSO satellites are

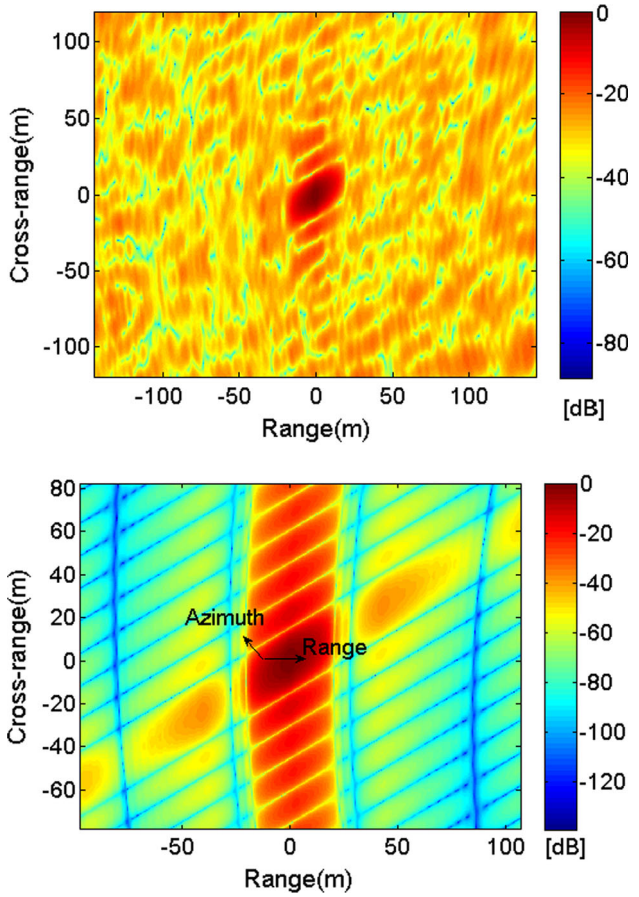

Fig. 9 Simulated images of a point target with 50 m^2 RCS in case of BeiDou IGSO satellite and a stationary receiver, where Gaussian white noise is added to verify the SNR (*top*), or no Gaussian white noise is added to verify the resolution (*bottom*)

Table 4 Theoretical and simulation results of SS-BSAR consisting of BeiDou IGSO satellite and a stationary receiver

	SNR (dB)	Range resolution (m)	Azimuth resolution (m)
Theoretical result	27.73	11.78	11.32
Simulation result	27.49	11.82	11.53

different from those of the MEO satellite, SS-BSAR with these two satellites as transmitters could provide some new potential applications compared with the well-described MEO transmitter, such as permanent and continuous monitoring of the targets, and the experimental demonstration of the GEO SAR (Hu et al. 2011). Furthermore, when the BeiDou GEO and IGSO satellites or other GNSS satellites are considered, and the system geometry and the parameters of the receiver keep the same as in the case of BeiDou MEO satellite, the differences in the SNR and the spatial resolution are concluded in Table 5. These analysis results can provide reference values for the multistatic SAR

Table 5 Performance difference of SS-BSAR using BeiDou GEO and IGSO satellites or other GNSS satellites as transmitters when compared to the BeiDou MEO transmitter

	BeiDou GEO	BeiDou IGSO	GPS L1 (C/A)	GLONASS L1 (P)	Galileo E5b (Q)
Airborne receiver					
SNR	Same	Same	Higher	Lower	Higher
Range resolution	Same	Same	Worse	Worse	Same
Azimuth resolution	Same	Same	Finer	Finer	Worse
Stationary receiver					
SNR	/	Higher	Same	Lower	Higher
Range resolution	/	Same	Worse	Worse	Same
Azimuth resolution	/	Worse	Finer	Finer	Worse

when different GNSS satellites are simultaneously used as transmitters.

It should be noted that besides SNR and resolution, other parameters are also important for the performance analysis of SS-BSAR, such as reliability and precision. Actually, SS-BSAR using GPS or GLONASS satellites as transmitter can achieve better reliability and precision than the BeiDou system, because the GPS and GLONASS systems have more available satellites and longer operating period. These parameters will become worse in case of the Galileo system, as this system is still at its infancy.

Acknowledgments The authors would like to thank the anonymous reviewers for their helpful comments. This work was supported in part by the Chinese Postdoctoral Science Foundation under Grant 2015T80834 and in part by the National Natural Science Foundation of China under Grant 41504007.

References

Antoniou M, Zeng Z, Feifeng L, Cherniakov M (2012) Experimental demonstration of passive BSAR imaging using navigation satellites and a fixed receiver. IEEE Geosci Remote Sens 9(3):477–481. doi:10.1109/LGRS.2011.2172571

Antoniou M, Hong Z, Zhangfan Z, Zuo R, Zhang Q, Cherniakov M (2013) Passive bistatic synthetic aperture radar imaging with Galileo transmitters and a moving receiver: experimental demonstration. IET Radar Sonar Navig 7(9):985–993. doi:10.1049/iet-rsn.2012.0330

BeiDou (2013) BeiDou navigation satellite system signal in space interface control document (Version 2.0).China satellite navigation office Dec 2013. http://www.beidou.gov.cn

Cherniakov M (2002) Space-surface bistatic synthetic aperture radar: prospective and problems. In: Proceedings of international conference on radar, Edinburgh, 15–17 Oct, pp 22–25

Cherniakov M, Saini R, Zuo R, Antoniou M (2007) Space-surface bistatic synthetic aperture radar with global navigation satellite system transmitter of opportunity: experimental results. IET Radar Sonar Navig 1(6):447–458. doi:10.1049/iet-rsn:20060172

He X, Cherniakov M, Zeng T (2005) Signal detectability in SS-BSAR with GNSS non-cooperative transmitter. IEE Proc Radar Sonar Navig 152(3):124–132. doi:10.1049/ip-rsn:20045042

Hu C, Long T, Zeng T, Liu F, Liu Z (2011) The accurate focusing and resolution analysis method in geosynchronous SAR. IEEE Trans Geosci Remote 49(10):3548–3563. doi:10.1109/TGRS.2011.2160402

Jin S, Feng GP, Gleason S (2011) Remote sensing using GNSS signals: current status and future directions. Adv Space Res 47(10):1645–1653. doi:10.1016/j.asr.2011.01.036

Lazarov A, Kostadinov T, Chen VC, Morgado JP (2013) Bistatic SAR system with GPS transmitter. In: IEEE radar conference (RADAR), Ottawa, 29 April–3 May, pp 1–6

Montenbruck O, Hauschild A, Steigenberger P, Hugentobler U, Teunissen P, Nakamura S (2013) Initial assessment of the COMPASS/BeiDou-2 regional navigation satellite system. GPS Solut 17(2):211–222. doi:10.1007/s10291-012-0272-x

Saini R, Zuo R, Cherniakov M (2008) Development of space-surface bistatic synthetic aperture radar with GNSS transmitter of opportunity. In: IEEE radar conference (RADAR), Rome, 26–30 May, pp 1–6

Saini R, Zuo R, Cherniakov M (2010) Problem of signal synchronization in space-surface bistatic synthetic aperture radar based on global navigation satellite emissions: experimental results. IET Radar Sonar Navig 4(1):110–125. doi:10.1049/iet-rsn.2008.0121

Skolnik MI (1990) Radar handbook. In: Cutrona LJ (ed) Synthetic aperture radar, 2nd edn. McGraw Hill, New York, pp 21.15–21.16

Woodward PM (1953) Probabilities and information theory, with application to radar. Pergamon Press, New York

Ye JH, Jiang YS, Zhao JZ, Guo JP (2011) Study of SAR imaging with BEIDOU signal. Sci China, Ser G 54(6):1051–1058. doi:10.1007/s11433-011-4335-8

Zeng T, Cherniakov M, Long T (2005) Generalized approach to resolution analysis in BSAR. IEEE Trans Aerosp Electron Syst 41(2):461–473. doi:10.1109/TAES.2005.1468741

Zeng T, Ao D, Hu C, Zhang T, Liu F, Tian W, Lin K (2015) Multiangle BSAR imaging based on BeiDou-2 navigation satellite system: experiments and preliminary results. IEEE Trans Geosci Remote 53(10):5760–5773. doi:10.1109/TGRS.2015.2430312

Shuzhu Shi is a lecturer in Wuhan University. He received his Ph.D. degree from Wuhan University in 2009. From 2009 to 2011, he was an Engineer with Nanjing Research Institute of Electronics Technology. From 2011 to 2015, he did his postdoctoral program in the Research Center of GNSS, Wuhan University. His current research interests include space-surface bistatic synthetic aperture radar (SAR) and GNSS-reflectometry.

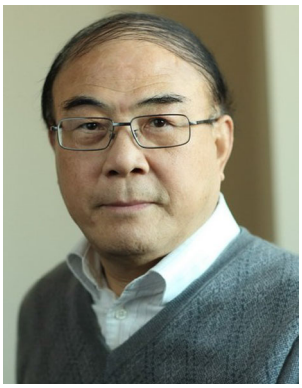

Jingnan Liu is a professor in Wuhan University. He received his M.S. degree in 1982. From 1998 to 2003, he was the Team Leader of the National Engineering Research Center for Satellite Positioning System. From 2003 to 2008, he was the President of Wuhan University. He has been a member of the Chinese Academy of Engineering since 1999, and been the President of Duke University, Kushan, China, since 2012. His current research interests include satellite precise orbit determination, GNSS-reflectometry, large-scale GNSS network adjustment theory and applications.

Tao Li is a professor in Wuhan University. He received his Ph.D. degree from Wuhan University in 2004. His current research interests include interferometric SAR technique and ground-based SAR.

Weiming Tian is a lecturer in the Beijing Institute of Technology (BIT). He received his Ph.D. degree from BIT in 2010. His current research interests include SAR system and signal processing.